Thermal and electromagnetic design of a DC HTS cable for the future French railway network

Ghazi Hajiri, Kévin Berger, Rémi Dorget, Jean Lévêque, Hervé Caron

Thermal and Electromagnetic Design of DC HTS Cables for the Future French Railway Network

Ghazi Hajiri, Kévin Berger, Rémi Dorget, Jean Lévêque, and Hervé Caron

***Abstract*— The use of High Temperature Superconducting (HTS) cables as a technology is considered as key to increasing the power of the electrical grid while reducing the volume of installation. In addition, when transmission currents exceed a few kA, DC HTS cables significantly reduce power losses, rights-of-way and total system mass. This article describes the various studies that need to be carried out in order to correctly size HTS DC cables for the new railway network envisaged by the French company SNCF, which must consider ultra-urban needs. The process used to design DC cables for operating powers of 10, 20 and 30 MW at a nominal voltage of 1.5 kV using commercial (RE)BCO tapes is presented. In this sizing process, the critical current density J_c(B, θ, T) dependence of the superconducting tapes, the thermal properties of the materials and the different cooling modes are taken into account. Several solutions are suggested to ensure that the cable can withstand fault currents and reduce recovery time in the initial state. Finally, with the help of analytical models and industrial data, once the cables have been designed, the various system losses are reported as well as the power or size of the various auxiliary components.**

***Index Terms*—Analytical models, Cryogenics, DC superconducting cable, Design tools, High-temperature superconductors, Magnetic fields, Thermal and hydraulic modelling.**

I. Introduction

DIRECT Current (DC) electrical networks represent a considerable portion of rail electrification in France and worldwide [1]. The transport of electrical energy in urban areas is limited by the space required for transformers and other static converters to transform electrical energy. Moreover, to reduce line losses, electrical energy is transported at high voltage, which requires a transformer substation close to where the energy is used, and the installation of a substation in a densely populated area imposes constraints. New environmental reforms also require a sharp reduction in electricity consumption [2], meaning that the French railway network has to adapt to these conditions.

In order to meet these constraints, recent developments in High Temperature Superconducting (HTS) tapes make it possible to develop cables carrying a high current density without losses [3]. Thus, the installation of a superconducting cable in an urban environment can be used to move substations to the periphery [4] where space constraints are lower and to transport electrical energy directly in the form in which it will be used, i.e. DC and low voltage. Moreover, the development of coated conductors such as (RE)BCO has undoubtedly provided a better current density than the first generation of HTS, BSCCO [5]-[6]. In addition to this, the price of (RE)BCO tapes is about €200/kA/m (according to a quotation issued in 2020 by Shanghai Superconductor Technology for a few km of 4 mm wide tapes), which is half the price of BSCCO tapes. This means that for the same cable length and price, twice as much current can be transmitted with coated conductors. Superconducting cables also have the advantage that they can be dimensioned to limit the current in case of a failure, e.g. short-circuit, overload [7].

The following section describe the sizing process of a superconducting installation for a DC cable, which always remains complex because of the numerous multiphysical constraints. In this article, a simple view of the algorithm is proposed to determine the necessary number of tapes per layer and per pole, while ensuring that the cable is protected in case of a fault. The performance of the algorithm does not stop at determining the number of superconducting tapes needed. Indeed, different design steps are discussed, and in particular the choice of cryogenic line, among which the following configurations feature: Concentric Pipes (CP), Separated Pipes (SP), and Concentric Pipes with Separated Return (CPSR), shown in Fig. 1. Therefore, the proposed design tool will also allow the selection of the cooling system and the required volume of the Liquid Nitrogen (LN_2) tank upstream of the installation. This volume is directly related to the targeted autonomy in LN_2, i.e. the time between two fillings t_{fill}, considering hydraulic losses P_{hyd}, cryostat heat losses P_{cryo}, contact resistances losses P_{cr}, and terminal losses P_{ter}.

II. Sizing Process

Before presenting our sizing method, we would like to specify that the cables studied here can be made up of several concentric layers placed in a liquid nitrogen pipe allowing cooling,

Manuscript receipt and acceptance dates will be inserted here. *(Corresponding author: Kévin Berger.)*

G. Hajiri, K. Berger, R. Dorget, J. Lévêque are with Université de Lorraine, GREEN, F-54000 Nancy, France (e-mail: name.surname@univ-lorraine.fr).

R. Dorget is also with Safran Tech, Electrical & Electronic Systems Research group, F-78114 Magny-Les-Hameaux, France (e-mail: remi.dorget@safrangroup.com).

H. Caron is with SNCF Réseau, F-93418 La plaine Saint Denis, France (e-mail: herve.caron@reseau.sncf.fr).

Color versions of one or more of the figures in this paper are available online at http://ieeexplore.ieee.org.

Digital Object Identifier will be inserted here upon acceptance.

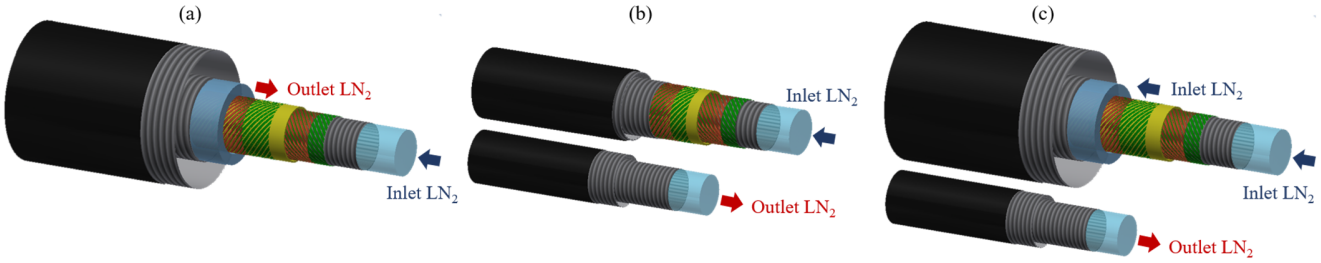

Fig. 1. Representation of cooling configurations: (a) Concentric Pipes (CP), (b) Separated Pipes (SP), and (c) Concentric Pipes with Separated Return (CPSR).

with the whole inserted into a cryostat. Fig. 2 shows a complete view of a superconducting coaxial cable with its different layers. The "Positive pole" located on top of the former consists of several superconducting tapes including an additional copper layer. The tapes are typically 4 mm in width and the thickness of the superconducting layer is about 1 µm, with a substrate thickness of 100 µm. The number of HTS tapes of the "pole" is closely related to the determination of the critical current of the cable. The next layer is composed of an electrical insulator to electrically separate positive and negative poles. Insulators such as Kraft paper soaked in liquid nitrogen are used. On the one hand, the impregnated Kraft paper has a high dielectric strength of 50 kV/mm [8], and on the other hand, if the nitrogen forms gas bubbles, its dielectric strength drops to 2-3 kV/mm [9]. For practical reasons, the insulation layer must be thick enough to not tear, i.e. a thickness of at least 2 mm. Next, a set of HTS tapes and copper constituting the negative pole is placed on top of the insulator, carrying the same current as the positive pole but in the opposite direction. All these layers are inserted into a cryostat to maintain the temperature of the cable below the vaporization point of the liquid nitrogen. Depending on the chosen architecture for the cooling of the cable, the liquid nitrogen outlet to the cooling station can be located either outside the cable, in a separate pipe, see Fig. 1 (b) and (c), or inside the cable (a). The algorithm used for the design of DC superconducting cables is proposed in Fig. 3. The input parameters are U_n and I_n, which are the operating voltage and current of the railway network respectively, I_f is the peak current that the Circuit Breaker (CB) has to cut off, t_f is the duration before the CB opens, and L is the length of the desired cable. DIN EN10380 is the international standard specifying the minimum requirements for the design, manufacture, testing and installation of corrugated flexible metal pipes and hoses. In this paper, the following parameters have been used: U_n = 1500 V, I_n = 6.67, 13.33 and 20 kA, I_f = 25 kA, t_f = 50 ms and L are between 500 m and 2000 m.

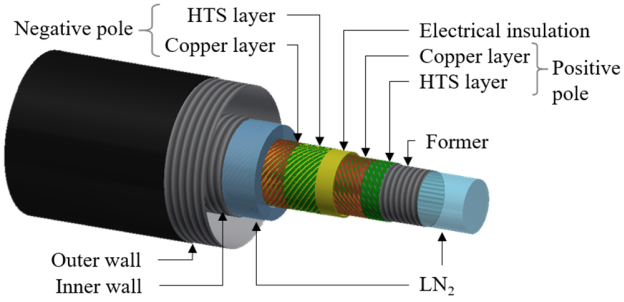

Fig. 2. Complete view of a superconducting coaxial cable with its different layers.

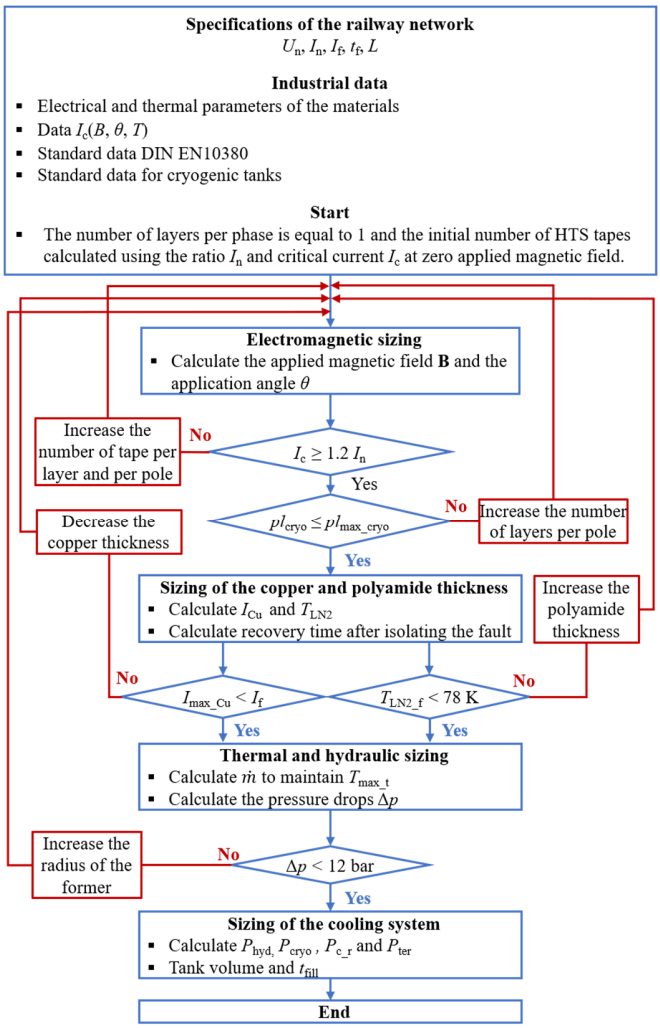

Fig. 3. The algorithm used for the design of DC superconducting cables: The electrical parameters of the railway network U_n and I_n are the operating voltage and current respectively, and L is the length of the cable, I_c is the critical current of the cable, pl_{cryo} and pl_{max_cryo} are respectively the cryostat losses and the maximum admissible cryostat losses per unit length, I_{Cu} is the current in the copper parts during a fault. T_{LN2_f} is the temperature of LN_2 in contact with the dissipating parts during a fault, $\dot{m}$ is the mass flow of liquid nitrogen. Other parameters will be explained in the following sections.

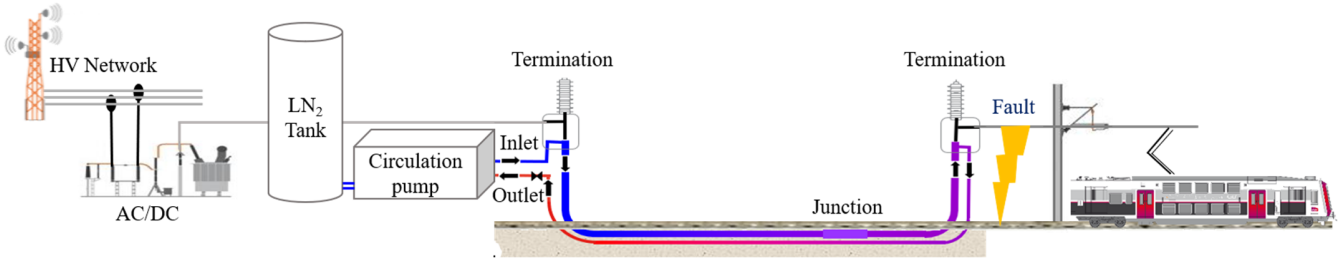

Fig. 4. Typical diagram of the introduction of a superconducting cable into the railway network and location of a fault.

The first part called “Electromagnetic sizing” consists of identifying the critical current that must be higher than the operating current by considering the different cable designs. For this, a 2D analytical model has been developed for the calculation of magnetic fields on the HTS tapes in the cable. The second part of this paper consists in determining the copper thickness th_{Cu} and the thickness of a polyamide layer th_{pol} to ensure the continuity of operation of the cable during a fault and its ability to limit the fault current, and also to satisfy a reasonable recovery time. The last part aims to study the thermal and hydraulic steady state in order to design the necessary cooling system. Both in normal operation and in case of a fault, the liquid nitrogen is maintained in the following range: 68 K ≤ T_{LN2} ≤ 78 K and 3 bar ≤ p ≤ 15 bar [10].

A. *Electromagnetic study*

The DC HTS cable under consideration consists of two concentric poles. The inner positive pole carries a current $+I$ and the outer pole carries a current $-I$, along the length of the cable. It is important to note that each pole may have a different number of layers and tapes. A layer consists of superconducting tapes and the radius of each layer is directly related to the number of tapes on top of it. We want to calculate the magnetic field distribution produced by l layers per pole of N_l tapes when the cable is in operation. Since we are focusing on the design of DC HTS cables, the current density J can be considered as uniformly distributed between the tapes and constant in each of the superconducting parts. In the developed analytical model, the magnetic field produced by the whole cable is obtained by superposition, translation and rotation of an infinitely long tape in a 2D coordinate system.

To determine the critical current, the radial and tangential components of the magnetic field applied on each tape without considering the field of the tape itself are calculated (same principle used for the characterization of the tapes). For each simulation, the amplitude and the application angle of the magnetic field generated by the current flowing through the cable is calculated. From these values and using the tape manufacturer's data [11], [12], the critical current is obtained according to the maximal operating temperature T_{max_t} in contact with the tapes. Inhomogeneities over the cable length are taken into account by choosing a security margin of 20 % between the nominal current I_n and the critical current [14], so that the critical current of the cable I_c must be greater than 1.2 I_n.

B. *Copper thickness design (in case of a fault)*

In a traditional railway network, copper conductors can handle the current in case of a fault. However, with DC HTS cables, in case of a fault as shown on Fig. 4, as soon as the fault current exceeds the critical current of the superconducting tapes, the current I_{Cu} penetrates the copper layer, which leads to heat generation by joule effect, and tends to increase the resistance of the conductors and thus of the cable. As indicated in [15], the reduction of the copper thickness th_{Cu} makes it possible to limit the fault current. This phenomenon has a great advantage: it is no longer necessary to increase the power of existing protection devices, thus saving costs and installation volume. The objective of this section is to design and determine the ideal copper thickness to minimize the fault current before the circuit breaker opens, while maintaining the nitrogen in its operating range. The non-linearity of the superconducting tapes has been considered, using the E-J power law with a critical current density that varies as a function of temperature [16]. The physical parameters of the superconducting and copper layers have been considered homogeneous over the length of the cable and the calculations are made according to the highest temperature of the cable in normal operation. The electrical parameters used for the French railway network are given in table 5 of [17].

An electrical model such as [18] coupled with a thermal node model such as [19], [20] were used to study the temperature of the different layers of superconducting tapes as well as in LN_2. The thermal model developed is only radial and does not consider the heat exchange in the longitudinal direction. In order to prevent any issue, the initial temperature used to calculate the transient behavior of the cable in case of a fault is the maximal temperature observed along its length in normal operation.

Fig. 5 shows simplified diagrams of the behavior of a superconducting cable in case of a fault with cooling based on a concentric pipe: (a) without polyamide layer, (b) with polyamide layer. When a fault occurs, the current starts to penetrate the copper layer and the temperature of the tapes rises rapidly and reaches about 10 K in a few milliseconds. It may change the LN_2 to a gaseous state. The presence of the latter decreases the heat exchange in the cable and in some cases may also cause a dielectric breakdown of the cable. For this reason, a new layer is necessary to decrease the temperature gradient between the nitrogen and the superconducting tape in case of a fault. Therefore, to limit the temperature rise of the liquid nitrogen during a fault, and to avoid the risk of gas bubble formation, a thin layer of polyamide of thickness th_{pol} has been added on the outer

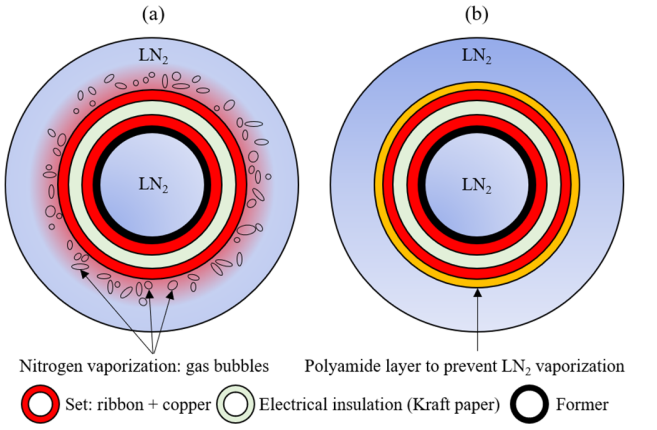

Fig. 5. Simplified diagrams of the behavior of a superconducting cable in case of a fault with cooling based on a concentric pipe: (a) without polyamide layer, (b) with polyamide layer.

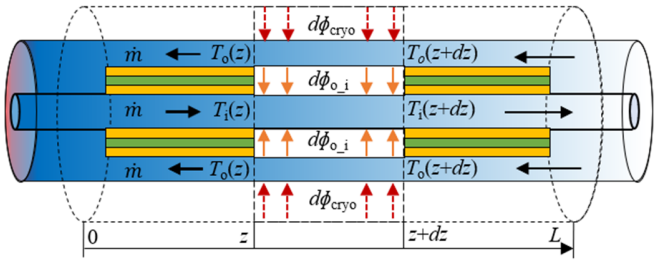

Fig. 6. Simplified sketch of the architecture of concentric pipes. $T_o(z)$ is the temperature in the outlet pipe and $T_i(z)$ the temperature in the inlet pipe. ϕ_{cyro} is the heat flow from the cryostat and ϕ_{o_i} is the heat flow transferred from the outlet pipe to the inlet pipe.

layer of the tapes, in direct contact with the liquid nitrogen. During the sizing process in case of a fault, the maximal temperature allowed for LN_2 is 78 K, which is 10 K below the boiling point at 3 bar. The thickness of this polyamide layer must be designed according to the characteristics of the fault, the length of the cable and the capabilities of the cooling station. By varying th_{pol}, the temperature difference between the dissipating parts and the liquid nitrogen during a fault can be adjusted. However, this thickness cannot be increased indefinitely, as this may greatly increase the recovery time t_r after the fault is isolated [21].

C. *Hydraulic and thermal design (normal operation)*

The main parameter concerning the thermal cooling of the cable is the LN_2 flow rate $\dot{m}$. The mass flow rate, in addition to being limited by the capacity of the station, is constrained by pressure drops Δp occurring in the pipe. Indeed, the circulation of a fluid in a long pipe induces strong pressure drops that can bring the LN_2 below the minimum pressure to maintain its liquid state and decrease both cooling and dielectric performances [22]. The main calculations are made using Bernoulli's theorem applied to each pipe. The pressure drops in the pipes are obtained by considering regular pressure drops [23] and using the Blasius correlation in order to estimate the coefficient of friction [24].

TABLE I
PARAMETERS OF THE DC HTS CABLES TO BE STUDIED

Parameter	Unit	Cable A	Cable B	Cable C
P_n	MW	10	20	30
U_n	kV	1.5	1.5	1.5
I_n	kA	6.67	13.33	20

In this section, the temperature of the tapes is calculated in the steady state along the cable length. For this thermal design, it is assumed that the only losses in the system are those introduced by the cryogenic lines and that they are proportional to the outer surface of the line. It is also assumed that the LN_2 temperature in a single pipe only varies with the length of the cable while the heat transfer between the layers is only in the radial direction. As illustrated in Fig. 6, a power balance is performed between z and $z+dz$, with dz an infinitesimal length. The temperature of LN_2 of each pipe along the length of the cable is then obtained by integration.

D. *Losses of a DC HTS cable installation*

In this section, the losses related to the superconducting cable and the losses related to the auxiliary components necessary for the operation of the entire cable are estimated. The architecture of the whole system is presented in Fig. 4. The losses of DC superconducting cables are mainly hydraulic losses and cryostat losses. At some junctions, the losses are mainly current-dependent; these are the losses related to the contact resistance. The values of contact resistances used in the design are of 200 and 800 $n\Omega.cm^{-2}$ for HTS tape to tape contact and HTS tape to copper contact, respectively [25]. The number of junctions has been chosen according to the length and radius of the cable and the dimensions of reel used to transport the cable to the installation area. The reel considered in our design has an outer diameter of 4.5 m, an inner diameter of 2.5 m and a width of 0.5 m.

A DC HTS cable requires two terminations making the connection with the conventional network at ambient temperature. For the calculation of termination losses, two categories are considered, heat losses and current-dependent losses. Heat losses are radiation losses and heat conduction losses, due to the temperature gradient at the ends of the current leads. Here, an ideal ratio between the length and cross section of the current lead has been chosen in order to obtain an equality between the joule losses and the conduction losses, i.e. 70 W/kA for 1 m of termination length.

III. RESULTS

The methods and models developed in the previous sections were used to size three DC superconducting cables. The characteristics of the studied cases are presented in Table I, where P_n is the nominal power of each cable. In this section, the design of the calculated cables is first shown, and the behavior of the cable in case of a fault will then be detailed. Finally, the best type of cooling is discussed as a function of the cable length and

other results are discussed such as the losses and the necessary amount of liquid nitrogen.

A. *Design of DC HTS cable*

For the three DC HTS cables shown in Table I, Fig. 7 shows the evolution of the number of tapes N and the inner wall diameter d_i of the cables as a function of the number of layers per pole l. When the number of layers per pole l is increased from one to two, the inner diameter d_i of the cable decreases sharply, by about 30 %. On the other hand, the total number of tapes N_t for 10, 20 and 30 MW cables are respectively 72, 142 and 208 for one layer and 92, 164 and 248 for two layers. Obviously, the number of necessary HTS tapes increases with the number of layers. This is mainly due to the increase in the perpendicular component of the magnetic field applied to the HTS tapes. This is why the calculation code developed in the electromagnetic sizing considers the variation in the number of tapes per layer in order to obtain the ideal number of tapes per pole as a function of the transport current. We can therefore conclude that there is a compromise to be found in the number of layers per pole in order to reduce both the outer diameter of the cable and the total number of necessary tapes. The major parameters for three DC HTS cables 500 m long after the sizing process are summarized in Table II. The black symbols in Fig. 7 also correspond to the final design of cables A, B and C for 500 m.

B. *Copper thickness design (in case of a fault)*

During a fault, the current flows inside the copper layer from the HTS tapes leave the superconducting state at the very beginning. In this part, the behavior of Cable A – 500 m has been studied in a short circuit for different thicknesses of the copper layer th_{Cu}. The appropriate choice of th_{Cu} mainly depends on the cable length and the protection devices of the network. In the framework of our study, typical Circuit Breakers (CB) in the SNCF network of 25 kA at peak and between 40 and 100 ms tripping time are used. This means that the maximal current during the fault I_{max_Cu} must be less than I_f = 25 kA. As mentioned before, the maximal temperature of the LN_2 in contact with the dissipating parts of the cable during the fault must also be less than 78 K in order to avoid bubbles in LN_2 and a dielectric breakdown in the cable. The behavior of the fault current during a short circuit for different copper thicknesses is shown in Fig. 8.

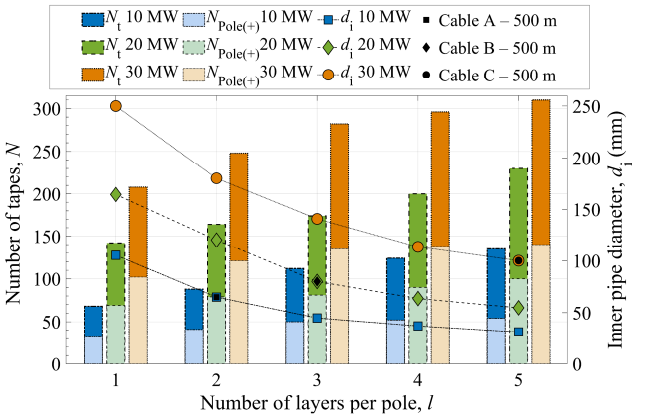

Fig. 7. Evolution of the number of tapes N and the inner wall diameter d_i of the cables as a function of the number of layers per pole l. N_t is the total number of tapes and $N_{Pole(+)}$ is the number of tapes for the "Positive pole" only.

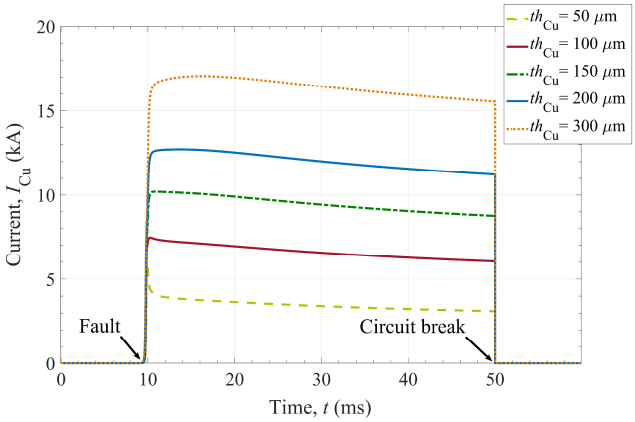

Fig. 8. Behavior of the fault current of Cable A – 500 m during a short circuit for different thicknesses of copper th_{Cu}.

TABLE II
MAJOR PARAMETERS OF THE DC HTS CABLES AFTER SIZING PROCESS

Parameter		Unit	Cable A – 500 m	Cable B – 500 m	Cable C – 500 m
Number of layers per pole			2	3	5
Standard former (inside/outside)		mm	25 (25.2 / 27.4)	32 (33.7 / 35.9)	32 (33.7 / 35.9)
Diameter of the layers	"Pole(+)"	mm	27.4 / 28.9	35.9 / 37.1 / 38.8	35.9 / 37.1 / 38.7 / 39.9 / 41.4
	"Pole(–)"		33.9 / 34.7	43.2 / 44.1 / 44.9	46.4 / 47.1 / 47.9 / 48.7 / 49.8
Number of tapes per layer	"Pole(+)"		20 / 21	26 / 27 / 28	26 / 27 / 28 / 29 / 30
	"Pole(–)"		23 / 24	30 / 31 / 32	32 / 33 / 34 / 35 / 36
Critical current of the tapes for each layer	"Pole(+)"	A	212 / 183	215 / 194 / 180	215 / 193 / 179 / 158 / 127
	"Pole(–)"		179 / 223	182 / 197 / 214	128/ 158 / 178 / 194 / 215
Standard diameter of inner pipe (inside/outside)		mm	65 (65/ 68.4)	80 (79.8 / 83.8)	100 (99.8 / 104.4)
Standard diameter of outer pipe (inside/outside)		mm	100 (99.8 / 104.4)	125 (125.6 / 130.8)	150 (151.9 / 157.9)

TABLE III
SET OF PARAMETERS OBTAINED FOR CABLE B – 500 M AFTER SIZING PROCESS FOR DIFFERENT TRIPPING TIMES

Parameter	Unit	CB1	CB2	CB3
t_f	ms	40	70	100
$I_{max\_Cu} = I_f$	kA	25	25	25
th_{Cu}	µm	150	150	150
th_{pol}	µm	310	430	550
T_{max_Cu}	K	115	127	136
t_r	s	53	74	92

In addition, Fig. 9 shows that it is very important to consider the variation in the electrical parameters of the cable as a function of temperature, as it varies a lot. Indeed, the temperature of the copper reaches more than 100 K in 40 ms. It can also be seen in Fig. 8 that the thinner the copper, the lower the peak of the fault current. This peak current is 17 kA, 13 kA, 10 kA, 7.5 kA, 6 kA for 300 µm, 200 µm, 150 µm, 100 µm, and 50 µm of copper, respectively. For each case, a polyamide layer about 300 µm thick ensures that T_{LN2_f} stays below 78 K. In case of a fault, it can be seen in Fig. 9 that a maximal copper temperature of 123 K is reached before the circuit break for a copper thickness of 50 µm. The recovery time t_r is the necessary time for the cable to recover the initial temperature after isolating the fault. t_r is 58 s, 49 s, 44 s, 38 s, 33 s for 300 µm, 200 µm, 150 µm, 100 µm, and 50 µm, respectively. Obviously, reducing the copper thickness also decrease the recovery time, which is also beneficial for the operation of DC HTS cable system.

Table III shows the set of parameters obtained after sizing Cable B – 500 m with three different tripping times t_f of 40, 70 and 100 ms and for the same peak of current during the fault equal to the current of the circuit breaker, i.e. I_f = 25 kA. The maximal temperature in the dissipative parts of the cable T_{max_Cu} is equal to 115, 127 and 136 K for t_f is equal to 40, 70 and 100 ms respectively. Indeed, this rise in temperature requires a thicker polyamide layer in order to maintain the nitrogen in the liquid state, which has an impact on the recovery time, i.e. t_r, respectively 53, 74 and 92 s for t_f of 40, 70 and 100 ms.

From our experience, the typical polyamide thickness th_{pol} is in the range of 200 to 800 µm. It mainly depends on the tripping time of the circuit breaker t_f, but a compromise must therefore be found in the thickness of the copper and the thickness of the polyamide layer to both limit the fault current and reduce t_r in order to meet the criteria of the rail network protection devices.

C. *Hydraulic and thermal design (normal operation)*

As an example, Fig. 10 shows the temperature distribution over the length of the cable B – 1.5 km in the steady state for different types of cooling. The selection of the appropriate cooling system can easily be made by considering the cost of the required pump, based on the necessary mass $\dot{m}$ and the pressure drop Δp. From a thermal point of view, it can be noted that the configuration of the concentric pipes (CP) requires a much lower cooling capacity since the difference between inlet and outlet temperature ΔT_{LN2} that the station has to cool down is much smaller than with separated pipes (SP), e.g. a ΔT_{LN2} of

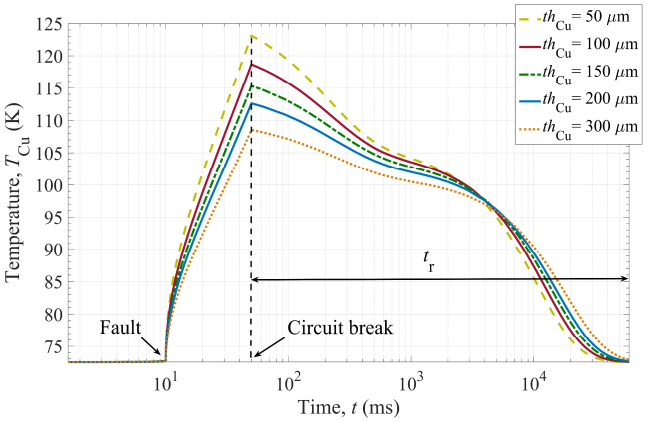

Fig. 9. Evolution of the temperature of the tapes of Cable A – 500 m before and after isolating the fault for different thicknesses of copper th_{Cu}.

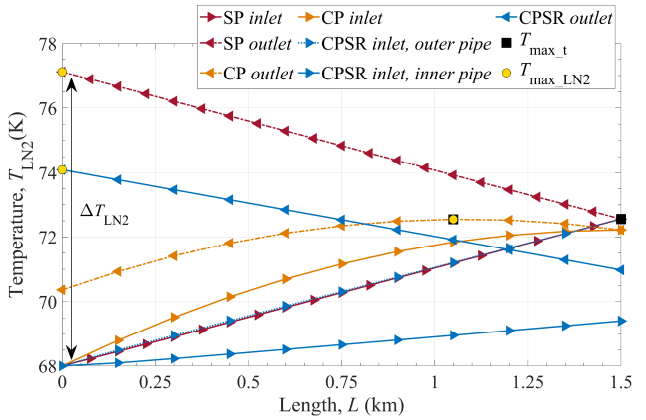

Fig. 10. Temperature distribution along the length of Cable B – 1.5 km. The mass flow rate requirements are 1 kg/s for CP and 0.4 kg/s for SP and CPSR. T_{max_LN2} is the maximal temperature of the LN_2 of the outlet and T_{max_t} is the maximal temperature of the liquid nitrogen along the cable in contact with the HTS tapes.

about 2.5 K is observed for CP and 9 K for SP. This is simply explained by the presence of two different cryostats for the separated pipes, which implies a larger external surface area, consequently generating more losses. T_{max_t} is the maximal temperature in contact with the HTS tapes that has been used to design the current capacities of the cable in the algorithm shown in Fig. 1. Thus, it should be noted that in order to maintain the same maximal temperature T_{max_t}, CP requires more powerful nitrogen circulation pumps than SP and CPSR. The interest of the CPSR and SP configurations compared to CP is that the hot point of the nitrogen T_{max_LN2} is not in contact with the HTS tapes, whereas in the CP configuration, T_{max_t} and T_{max_LN2} are the same. In addition, the location of T_{max_t} is difficult to control for CP, as it cannot be measured directly from the cable ends.

Fig. 11 and Fig. 12 show the evolution of the mass flow rate and pressure drop vs the length of Cable C for the three different configurations of cooling. It should be mentioned that the inner pipe diameter is 32 mm and the diameter of the outer pipe has been chosen to obtain the same hydraulic diameter as the inner pipe, i.e. 100 mm.

The length of the cable has a significant influence on the best choice for the type of cooling. Indeed, for a length of 1 km, the

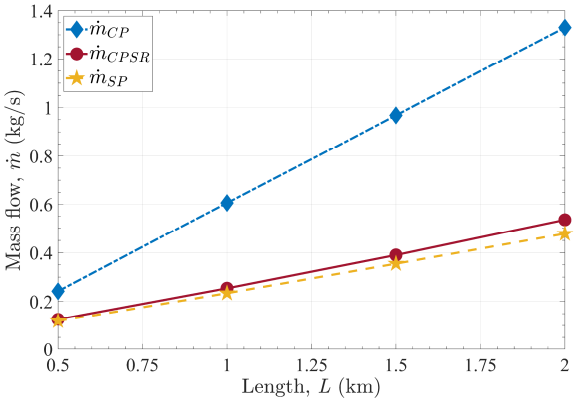

Fig. 11. Mass flow vs length of the Cable C for the three types of cooling CP, SP and CPSR in order to maintain T_{max_t} = 73 K and T_{max_LN2} below 78 K with an inlet pressure of 15 bar.

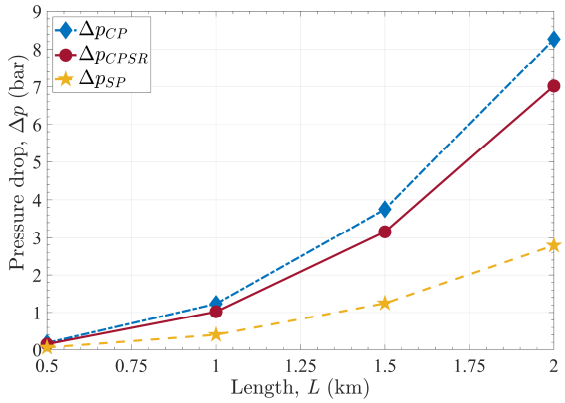

Fig. 12. Pressure drop vs length of the Cable C for the three types of cooling CP, SP and CPSR in order to maintain T_{max_t} = 73 K and T_{max_LN2} below 78 K with an inlet pressure of 15 bar.

necessary flow rate for CP is 0.6 kg/s with a pressure drop of about 1.5 bar, and it increases up to 1.35 kg/s generating a pressure drop of 8.2 bar for a 2 km length cable. The CP architecture therefore allows low heat losses for short lengths, but it is not suitable for long lengths, as this type of cooling requires an increase in the mass flow rate, which cannot be increased indefinitely as it risks leading to a sharp increase in friction inside the pipes.

It can also be seen that CPSR and SP require approximately the same flow rate to cool the cable. However, Fig. 12 shows that CPSR generates more pressure drop than SP, which is due to the fluid contact surface of the CPSR being larger than SP, generating more friction.

We would like to mention that the SP cooling was excluded from our cable selection despite its cooling efficiency and negligible pressure drop. Indeed, with SP, the cable is only cooled through the inner pipe, Fig. 1, which means that the recovery time after a fault might be very high, in particular for long length cables.

The CPSR ensures a low mass flow rate even for long lengths, i.e. a mass flow rate of 0.54 kg/s and a pressure drop of less than 7.02 bar for a length of 2 km. Although the CPSR requires the addition of a second external line for nitrogen return, this architecture is best suited to long cable lengths. Table IV presents the thermal and hydraulic parameters of the three cables in normal operation. The length of the cables has been chosen to present the most relevant results and variations: Cable A – 500 m, Cable B – 1000 m, and Cable C – 2000 m.

TABLE IV
THERMAL AND HYDRAULIC PARAMETERS IN NORMAL OPERATION

Parameter	Unit	Cable A – 500 m	Cable B – 1000 m	Cable C – 2000 m
Type of cooling		CP	CP	CPSR
$\dot{m}$	kg/s	0.254	0.595	0.536
Δp	bar	0.192	1.267	7.019

TABLE V
LOSSES OF THE INSTALLATION AND CHARACTERISTICS OF THE COOLING SYSTEM OF THE THREE CABLES

Parameter	Unit	Losses		
		Cable A – 500 m	Cable B – 1000 m	Cable C – 2000 m
P_{hyd}	W	7	93	448
P_{cryo}	W	746	1 524	3 173
P_{c_r}	W	636	754	1 146
P_{ter}	W	2 104	3 840	5 380
P_{tot}	W	3 493	6 211	10 147
		LN_2		
Q_{LN2}	L/h	114.95	201.36	320.55
N_p		2	2	3
P_p	W	3 500	6 500	5 500
		Tank		
Volume	L	61.62	80.36	80.36
Height	m	14.15	18.05	18.05
Diameter	m	3	3	3
Losses	%	0.21	0.21	0.21
t_{fill}	day	7	6	4

P_{tot} are the total losses of the superconducting installation. Q_{LN2} is the quantity of LN_2 consumed. N_p is the necessary number of circulation pumps. One circulation pump is always added for the continuity of service in case of failure of the operational pump-s). P_p is the power of a single pump.

D. *DC HTS system losses*

In order to size the three superconducting cables shown in Table IV, the losses were calculated in each case, and summarized in Table V. The consumption of liquid nitrogen and the power required for the circulation pumps are also mentioned. The role of the latter is to compensate for the losses of the installation. Of course, the greater the length or the current of the cable, the more the installation requires cooling power. That is, a power of about 3.5 kW for Cable A, 6.5 kW and 11 kW for Cables B and C respectively. It is also advisable to install two pumps in parallel to ensure the continuity of service of the entire system [26]-[27]. In the case of Cable C, three pumps are required, two of them running in parallel during normal operation while the third one ensures continuity of service. The sizing of a subcooler is relatively complex and requires a dedicated study by refrigeration experts. This study has not been carried out here but it can be mentioned that an electrically and thermally

reliable subcooler usually has three vacuum pumps, two operating at half their rated power and the third pump operating only when one pump is being serviced. The consumption of liquid nitrogen is related to total losses, including tank losses. This consumption is used to determine the volume of the required liquid nitrogen tank. The amount of nitrogen in the tank must not exceed 85 % of its total volume to maintain the nitrogen under pressure, and less than 45 % to ensure continuity in case of a filling incident or delay. The time between two fillings t_{fill} can be determined from these constraints.

IV. Conclusion

This article shows a method for sizing superconducting cables as well as the various auxiliary components in a DC superconducting installation. Multi-physical analytical models were developed in order to guarantee an approach that meets the criteria of the French railway network.

This strategy includes an electromagnetic sizing for the determination of the critical current, associated with a hydraulic and thermal dimensioning in normal operation to determine the best type of cable cooling. The proposed sizing process also protects the HTS cable in case of a fault. A solution is proposed consisting in finding a compromise between the thickness of the copper layer to support a flow of a given fault current (related to the circuit breaker) and maintain the nitrogen in its liquid state. A solution which consists in increasing the number of layers per pole is also studied here in order to reduce the outer radius of the cable. Nevertheless, this strategy reduces the critical current of the tapes due to a higher applied magnetic field on the HTS tapes.

The increase in cable length requires higher mass flow rates, which leads to bigger cooling stations and increasingly powerful pumps. The performance of our code does not stop at the dimensioning of the cable; it allows the calculation of the diameter of cryogenic pipes in accordance with DIN EN 10380. In other words, the sizing of DC HTS cables including the sizing of nitrogen pipes, nitrogen tanks and circulation pumps already exists on the European market.

References

[1] H. Ohsaki, Z. Lv, N. Matsushita, M. Sekino, T. Koseki, and M. Tomita, "Superconducting Power Cable Application in DC Electric Railway Systems," *IEEE Transactions on Applied Superconductivity*, vol. 23, no. 3, pp. 3600705–3600705, Jun. 2013, doi: 10.1109/TASC.2013.2237874.

[2] E. Kriegler, "Long-term transport energy demand and climate policy: Alternative visions on transport decarbonization in energy-economy models," *Energy*, Accessed: Aug. 22, 2020. [Online]. Available: https://www.academia.edu/31708284/Long_term_transport_energy_demand_and_climate_policy_Alternative_visions_on_transport_decarbonization_in_energy_economy_models.

[3] J. Oestergaard, J. Okholm, K. Lomholt, and O. Toennesen, "Energy losses of superconducting power transmission cables in the grid," *IEEE Transactions on Applied Superconductivity*, vol. 11, no. 1, pp. 2375–2378, Mar. 2001, doi: 10.1109/77.920339.

[4] M. Stemmle *et al.*, "Three years operation experience of the AmpaCity system installation in Essen, Germany," p. 22.

[5] X. Obradors and T. Puig, "Coated conductors for power applications: materials challenges," *Supercond. Sci. Technol.*, vol. 27, no. 4, p. 044003, Apr. 2014, doi: 10.1088/0953-2048/27/4/044003.

[6] S. Samoilenkov *et al.*, "Customised 2G HTS wire for applications," *Supercond. Sci. Technol.*, vol. 29, no. 2, p. 024001, Feb. 2016, doi: 10.1088/0953-2048/29/2/024001.

[7] H. Kojima, F. Kato, N. Hayakawa, M. Hanai, and H. Okubo, "Superconducting Fault Current Limiting Cable (SFCLC) with Current Limitation and Recovery Function," *Physics Procedia*, vol. 36, pp. 1296–1300, 2012, doi: 10.1016/j.phpro.2012.06.293.

[8] A. Masood, M. U. Zuberi, and E. Husain, "Breakdown strength of solid dielectrics in liquid nitrogen," *IEEE Transactions on Dielectrics and Electrical Insulation*, vol. 15, no. 4, pp. 1051–1055, Aug. 2008, doi: 10.1109/TDEI.2008.4591227.

[9] D. Gromoll, R. Schumacher, and C. Humpert, "Dielectric strength of insulating material in LN $_2$ with thermally induced bubbles," *J. Phys.: Conf. Ser.*, vol. 1559, p. 012087, Jun. 2020, doi: 10.1088/1742-6596/1559/1/012087.

[10] "M. Noe, 'Superconducting_Cables,' presented at the EUCAS Short Course Power Applications, Geneva, 17-Sep-2017."

[11] S. C. Wimbush and N. M. Strickland, "A Public Database of High-Temperature Superconductor Critical Current Data," *IEEE Transactions on Applied Superconductivity*, vol. 27, no. 4, pp. 1–5, Jun. 2017, doi: 10.1109/TASC.2016.2628700.

[12] S. Wimbush and N. Strickland, "A high-temperature superconducting (HTS) wire critical current database," Oct. 2019, doi: 10.6084/m9.figshare.c.2861821.v10.

[13] M. S. N, H. C, and C. W. S, "A high-temperature superconducting (HTS) wire critical current database A https://figshare.com/collections/A_high_temperature_superconducting_HTS_wire_critical_current_database/2861821/10." https://figshare.com/collections/A_high_temperature_superconducting_HTS_wire_critical_current_database/2861821 (accessed Feb. 03, 2020).

[14] M. Solovyov *et al.*, "Non-uniformity of coated conductor tapes," *Supercond. Sci. Technol.*, vol. 26, no. 11, p. 115013, Nov. 2013, doi: 10.1088/0953-2048/26/11/115013.

[15] H. J. Kim, J. W. Shim, K. Sim, and K. Hur, "Assessment of Improved Power Quality Due to Fault Current Limiting HTS Cable," *IEEE Transactions on Applied Superconductivity*, vol. 23, no. 3, pp. 5602104–5602104, Jun. 2013, doi: 10.1109/TASC.2012.2235500.

[16] J. Duron, F. Grilli, B. Dutoit, and S. Stavrev, "Modelling the E–J relation of high-Tc superconductors in an arbitrary current range," *Physica C: Superconductivity*, vol. 401, no. 1–4, pp. 231–235, Jan. 2004, doi: 10.1016/j.physc.2003.09.044.

[17] M. Tomita *et al.*, "Train Running Test Transmitted by Superconducting Feeder Cable and Study as an Example of Line in Japan and France," *IEEE Transactions on Applied Superconductivity*, vol. 30, no. 2, Art. no. 2, Mar. 2020, doi: 10.1109/TASC.2019.2949237.

[18] S. Venuturumilli, F. Berg, L. Prisse, M. Zhang, and W. Yuan, "DC Line to Line Short-Circuit Fault Management in a Turbo-Electric Aircraft Propulsion System Using Superconducting Devices," *IEEE Transactions on Applied Superconductivity*, vol. 29, no. 5, pp. 1–6, Aug. 2019, doi: 10.1109/TASC.2019.2909206.

[19] W. T. B. de Sousa, A. Polasek, R. Dias, C. F. T. Matt, and R. de Andrade, "Thermal–electrical analogy for simulations of superconducting fault current limiters," *Cryogenics*, vol. 62, pp. 97–109, Jul. 2014, doi: 10.1016/j.cryogenics.2014.04.015.

[20] N. Rostami, M. R. Feyzi, J. Pyrhonen, A. Parviainen, and M. Niemela, "Lumped-Parameter Thermal Model for Axial Flux Permanent Magnet Machines," *IEEE Transactions on Magnetics*, vol. 49, no. 3, pp. 1178–1184, Mar. 2013, doi: 10.1109/TMAG.2012.2210051.

[21] T. Rubeli, D. Colangelo, B. Dutoit, and M. Vojenciak, "Heat transfer monitoring between quenched high-temperature superconducting coated conductors and liquid nitrogen," *Progress in Superconductivity and Cryogenics*, vol. 17, no. 1, pp. 10–13, 2015, doi: 10.9714/psac.2015.17.1.010.

[22] "'NEXANS. Superconducting cable systems. https://www.nexans.de/eservice/Germany- de_DE/fileLibrary/Download_540144810/Germany/files/Nexans_Superconducting_cable_systems.pdf,' Hannover, Nexans Deutshcland GmBH."

[23] W. T. B. de Sousa, D. Kottonau, J. Bock, and M. Noe, "Investigation of a Concentric Three-Phase HTS Cable Connected to an SFCL Device," *IEEE Transactions on Applied Superconductivity*, vol. 28, no. 4, pp. 1–5, Jun. 2018, doi: 10.1109/TASC.2018.2794586.

[24] "K. T. Trinh, 'On the Blasius correlation for friction factors,' ArXiv10072466 Phys., Jul. 2010."
[25] N. Bagrets, A. Augieri, G. Celentano, G. Tomassetti, K.-P. Weiss, and A. della Corte, "Investigation of ReBCO Conductor Tape Joints for Superconducting Applications," *IEEE Transactions on Applied Superconductivity*, vol. 25, no. 3, pp. 1–5, Jun. 2015, doi: 10.1109/TASC.2014.2373055.
[26] H. Yumura *et al.*, "Update of YOKOHAMA HTS Cable Project," *IEEE Transactions on Applied Superconductivity*, vol. 23, no. 3, pp. 5402306–5402306, Jun. 2013, doi: 10.1109/TASC.2013.2245931.
[27] X. Zong, D. Wei, Y. Han, and T. Tang, "Development of 35 kV 2000 A CD HTS Cable Demonstration Project," *IEEE Transactions on Applied Superconductivity*, vol. 26, no. 7, pp. 1–4, Oct. 2016, doi: 10.1109/TASC.2016.2598490.